Applied Catalysis B: Environmental 154–155 (2014) 369–378

Contents lists available at ScienceDirect

Applied Catalysis B: Environmental

journal homepage: www.elsevier.com/locate/apcatb

Water as solvent in the liquid-phase selective hydrogenation of crotonaldehyde to crotyl alcohol over Pt/ZnO: A factorial design approach

Jesús Hidalgo-Carrillo[a,1], Alberto Marinas[a], José M. Marinas[a], Juan J. Delgado[b], Rocío Raya-Miranda[c], Francisco J. Urbano[a,*]

[a] Departamento de Química Orgánica, Universidad de Córdoba, Campus de Excelencia Agroalimentario (ceiA3), Campus de Rabanales, Marie Curie Buiding, E-14014, Córdoba, Spain
[b] Departamento de Ciencia de Materiales e Ingeniería Metalúrgica y Química Inorgánica, University of Cadiz. Campus Río San Pedro s/n 11510, Puerto Real, Spain
[c] Dpto. Estadística e Investigación Operativa. Facultad de Ciencias. Universidad de Granada. Campus Fuentenueva, E-18071 Granada, Spain

ARTICLE INFO

Article history:
Received 19 December 2013
Received in revised form 6 February 2014
Accepted 12 February 2014
Available online 21 February 2014

Keywords:
Pt/ZnO
Water as solvent
Crotonaldehyde selective hydrogenation
Crotyl alcohol
Factorial design

ABSTRACT

The liquid-phase selective reduction of crotonaldehyde to crotyl alcohol was studied on Pt/ZnO. Optimization through factorial design of experiments led to a 75% increase in the yield to crotyl alcohol and solvent was found to be the most influential parameter. The yield to the unsaturated alcohol was found to increase with the water content in water/dioxane mixtures. FT-Raman spectroscopy evidenced the progressive weakening of C=O bond as the water content was increased thus accounting for the catalytic results. A study of catalyst reutilization showed an increase in both conversion and selectivity up to the third use, subsequent reuses leading to a drop in both parameters. The data obtained by XRD, XPS, and HAADF showed that the evolution of chlorinated species in the catalytic system were the plausible cause of this behavior.

1. Introduction

Selective hydrogenation of C=O bond in α,β-unsaturated carbonyl compounds leads to olefinic alcohols of interest in Pharmaceutical and Fragance Industries though the process is thermodinamically unfavored (hydrogenation of C=C is favored over C=O by ca. 35 kJ/mol) [1]. The most widely used catalysts for the process are group VIII metals [2–4], and in particular platinum. Furthermore, in order to enhance activity and selectivity to unsaturated alcohol, different strategies have been described such as the addition of a second 3d metal [5,6], or the use of (partially) reducible supports (TiO_2, ZnO, etc.) to promote strong metal-support interactions (SMSI) and eventually alloy formation [7–12]. All these strategies are aimed at weakening the C=O bond and/or avoiding the adsorption through C=C bond.

Pt/ZnO [6,9,13,14] has been found to be one of the most selective systems to yield unsaturated alcohol, which has been partly attributed to the formation of a Pt–Zn alloy, as evidenced by the shift in the Pt^0 X-ray diffraction band or the narrowing of Pt XPS lines upon reduction at 200–400 °C [13,14]. Nevertheless, in a previous work [9], we studied the catalytic performance of a Pt/ZnO system obtained using H_2PtCl_6 as the metal precursor. Interestingly, the system reduced at 175 °C, in which no Pt–Zn alloy was observed by XRD exhibited similar selectivity to but-2-en-1-ol (95%) as that activated at 400 °C whereas conversion was significant higher (10.6% and 4.7% for Pt/ZnO-175 and Pt/ZnO-400, respectively) under similar reaction conditions. Given the fact that metal particle sizes were not very different, structural changes associated to the evolution of chloride species coming from the precursor were postulated as an additional factor to account for such catalytic performance.

In fact, the platinum precursor has an important influence on catalytic performance of Pt/ZnO systems. Therefore, Ammari et al. [13] found that when H_2PtCl_6 had been used as the precursor (as it was our case), the resulting catalyst was much more active and selective as compared to the use of $Pt(NH_3)_4(NO_3)_2$. The authors explained such a significant improvement in terms of selective adsorption of C=O on Lewis acid sites of ZnOxCly species localized

* Corresponding author. Tel.: +34 957218638; fax: +34 957212066.
E-mail address: FJ.Urbano@uco.es (F.J. Urbano).
[1] Present address: Department of physical chemistry, Faculty of Chemical Technology, University of Pardubice, Pardubice, Czech Republic.

http://dx.doi.org/10.1016/j.apcatb.2014.02.023
0926-3373/

on the support in the vicinity of PtZn particles. It is evident that for this catalytic system, determination of chlorine environments and its evolution with the different reaction conditions would be highly desirable in order to elucidate its influence on catalytic performance, though this is not an easy task due to its low concentration [15]. In an attempt at determining such Cl distribution, Wang et al. [15] resorted to EDX and element mapping in STEM which allowed them to postulate the existence of zinc chloride or oxychlorinated species of zinc.

Once a catalyst has been selected, there are some other variables influencing catalytic performance in hydrogenation reactions such as temperature, hydrogen pressure or reaction medium (for processes conducted in the liquid-phase), just to cite some of them. In this sense, for process optimization, in order to avoid to study the effect of one of these variables on conversion and selectivity at a time, but to consider their possible interdependence, factorial design can be used which also reduces the required experimental testing considerably [16]. Factorial design of experiments has been successfully used in heterogeneous catalysis, especially in biocatalysis [17–19].

In the present piece of research, the operational reaction conditions such as water content on solvent mixtures, the reaction temperature and the initial hydrogen pressure were optimized by factorial design in order to maximize both crotonaldehyde conversion and the amount of unsaturated alcohol produced (yield of but-2-en-1-ol). Moreover, new XPS evidences for the crucial role of ZnOxCly species in liquid-phase selective hydrogenation of crotonaldehyde to crotyl alcohol on Pt/ZnO are given and a plausible explanation of the observed differences in catalytic behavior on reduction temperature and reutilization experiments is presented.

2. Experimental

2.1. Catalyst synthesis

The catalysts studied were obtained from an aqueous solution containing 8% (w/w) chloroplatinic acid (Sigma–Aldrich Ref. 262587) as metal precursor and zinc (II) oxide (Sigma–Aldrich Ref. 544906) as the support.

The synthetic procedure was as follows: a volume of 6.57 mL of chloroplatinic acid solution was diluted to 200 mL with Milli-Q water and adjusted to pH 7 by adding 0.1 M NaOH (FLUKA Ref. 43617). Then, an amount of 4.75 g of support was added and the mixture readjusted to pH 7 with HCl. The solution containing the support was refluxed at 80 °C under vigorous stirring for 2 h. Then, a volume of 10 mL of isopropanol was added, the temperature rose to 110 °C and refluxing continued for 30 min, after which the mixture was vacuum filtered and the filtrate washed with three portions of 25 mL of water each. The resulting solid was dried in a muffle furnace at 110 °C for 12 h, ground and calcined at 400 °C for 4 h. After calcination, the solid was ground again, sieved through a mesh of 0.149 mm pore size and stored in a topaz flask. The nominal proportion of Pt in the catalyst thus obtained was 5 wt%. Finally, the catalyst was reduced under a hydrogen stream flowing at 30 mL/min at selected temperatures for 2 h. Reduction temperature was chosen according to significant features observed in the temperature-programmed reduction profiles [9].

The solid names include the metal, its support and the reduction temperature used (*i.e.* Pt/ZnO-unred, Pt/ZnO-175, Pt/ZnO-400, for the systems used as synthesized or reduced at 175 °C and 400 °C, respectively).

2.2. Catalyst characterization

Elemental analysis of Pt/ZnO was performed by the staff at the Central Service for Research Support (SCAI) of the University of Córdoba, using inductively coupled plasma-mass spectrometry (ICP-MS). Measurements were made on a Perkin–Elmer ELAN DRC-e instrument following dissolution of the sample in a 1:1:1 H_2SO_4/HF/H_2O mixture. Calibration was done by using PE Pure Plus atomic spectroscopy standards, also from Perkin–Elmer.

EDX measurements were made with a JEOL JSM-6300 scanning electron microscope (SEM) equipped with an energy-dispersive X-ray (EDX) detector at the SCAI of the University of Cordoba.

Surface area of ZnO and Pt/ZnO were determined from nitrogen adsorption–desorption isotherms obtained at liquid nitrogen temperature on a Micromeritics ASAP-2010 instrument, using Brunnauer–Emmett–Teller (BET) method. Samples were degassed to 0.1 Pa at 110 °C prior to measurement.

High-resolution transmission (HRTEM) and high-angle annular dark-field scanning-transmission (HAADF-STEM) micrographs were obtained using a JEOL-2010F microscope available at University of Cádiz equipped with a field emission gun and operated at an acceleration voltage of 200 kV. The structural resolution of the equipment in the HRTEM mode was 0.19 nm at the Scherzer defocus conditions, while the diameter of the probe used in STEM was 0.5 nm.

X-ray patterns for the samples were obtained with a Siemens D-5000 diffractometer equipped with a DACO-MP automatic control and data acquisition system. The instrument was used with Co K_α radiation and a graphite monochromator.

X-ray photoelectron spectroscopy (XPS) data were recorded on 4 mm × 4 mm pellets 0.5 mm thick that were obtained by gently pressing the powdered materials following outgassing to a pressure below about 2×10^{-8} Torr at 150 °C in the instrument pre-chamber to remove chemisorbed volatile species. The main chamber of the Leibold-Heraeus LHS10 spectrometer used, capable of operating down to less than 2×10^{-9} Torr, was equipped with an EA-200MCD hemispherical electron analyser with a dual X-ray source using Al K_α ($h\nu$ = 1486.6 eV) at 120 W, at 30 mA, with C (1s) as energy reference (284.6 eV).

FT-Raman spectra were obtained on a Perkin–Elmer 2000 NIR FT-Raman system equipped with a diode pumped NdYAG laser (9394.69 cm^{-1}) that was operated at 500 mW laser power and a resolution of 4 cm^{-1} throughout the 3500–200 cm^{-1} range in order to gather 64 scans. Nevertheless, represented region corresponds to the 1750–1600 cm^{-1} range.

2.3. Hydrogenation experiments

The liquid-phase hydrogenation of crotonaldehyde with molecular hydrogen was conducted on a Parr Instruments 3911 low-pressure reactor, using a constant rate of 300 shakes min^{-1}. The reaction vessel (500 mL in volume) was wrapped in a metal jacket through which thermostated water was circulated. The apparatus was equipped with a gauge that recorded the pressure inside the reaction vessel throughout the experiment. All reactions were performed with an overall liquid volume of 20 mL containing 0.5 M crotonaldehyde in the selected solvent (dioxane, water or dioxane/water mixture in a 33.33%/66.66%, 50%/50% or 66.66%/33.33%, v/v ratio), using an initial pressure of 20, 50 or 80 psi and a temperature of 20, 50 or 80 °C, according to the experimental design created by StatGraphics® version 5.1. Prior to each run, an amount of 100 mg of calcined Pt catalyst was reduced in a hydrogen stream flowing at 30 mL/min at the selected temperature for 2 h and then cooled in the same stream. The standard operational procedure used in each experiment was as follows: the reaction vessel was loaded with 20 mL of 0.5 M crotonaldehyde and 100 mg of reduced catalyst, and sonicated for 15 min. The reaction vessel was then attached to the reactor and, once the temperature reached 20, 50 or 80 °C – which took about 10 min – the vessel was evacuated and filled with hydrogen to a pressure of 0.414 MPa twice. After

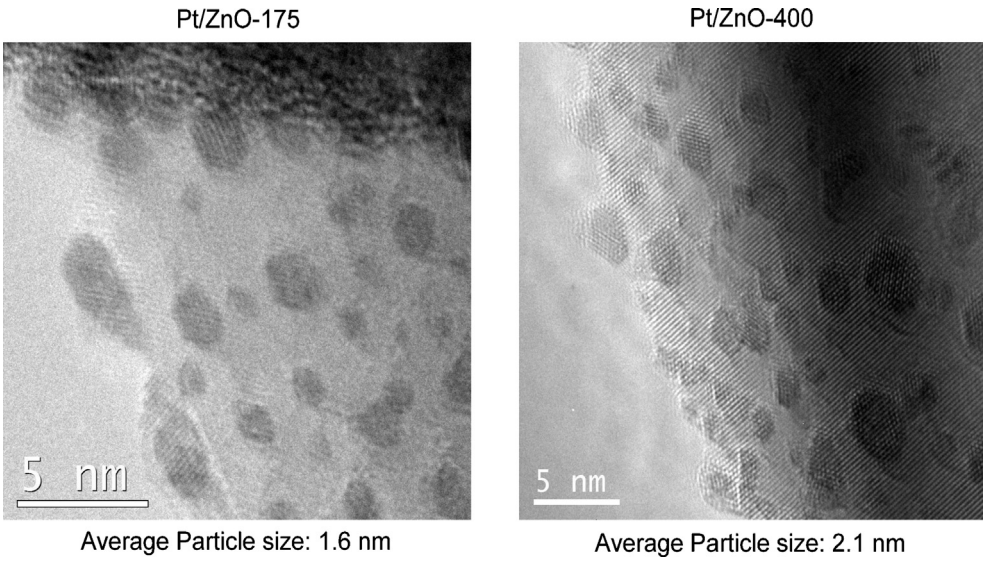

Fig. 1. TEM images of Pt/ZnO-175 and Pt/ZnO-400.

15 min, the pressure was readjusted, the shaking device started and the reaction timed. Blank tests intended to ascertain that no reaction would take place thermally in the absence of catalyst were conducted with a reaction mixture consisting solely of substrate and solvent. No signs of reaction were detected after 8 h under these conditions. Reaction products were analyzed on an Agilent gas chromatograph equipped with a flame ionization detector (FID) and a Supelcowax-10 column (30 m long × 0.25 mm ID, 0.25 μm film thickness). A calibration plot for each product was constructed from commercially available standards. The products of the reduction of crotonaldehyde were crotyl alcohol (but-2-en-1-ol), butan-1-ol and butanal. Both gas and liquid phase were analyzed and both phases are included in conversion and selectivity results.

2.4. Multifactorial design of experiments

The effect of process parameters (temperature, hydrogen pressure and solvent) on conversion and selectivity to but-2-en-1-ol on Pt/ZnO-175 was studied using a multifactorial design of experiments run by the software StatGraphics® version 5.1. Matrix design was randomized in order to eliminate the influence of any other non-observed co-variables on obtained results. Three factors were included in the factorial design: Temperature at three levels (20, 50 and 80 °C), Initial hydrogen pressure at three levels (20, 50 and 80 psi) and solvent at four levels (0, 33.33, 66.66 and 100% content and 100% water content in water/dioxane mixtures). The overall design, expressed as $\{3^2 \times 4^1\}$, involved 36 runs (Suplementary material, Table S1).

3. Results and discussion

3.1. Catalyst characterization

In a previous study [9], some of the features concerning characterization of Pt/ZnO-unred, Pt/ZnO-175 and Pt/ZnO-400 were described. Therefore, they are just summarized here laying emphasis on the new technique (HAADF) used and on the more in-detail characterization by XPS, key technique for determination of the evolution of chlorinated species.

ICP-MS analysis of Pt/ZnO showed a Pt content of 5.1% by weight, quite close to the nominal value (5%) thus evidencing a good incorporation of the metal. Pt surface content as determined by SEM-EDX was slightly lower (4%). Regarding surface area, incorporation of platinum led to an increase from 11 m^2/g (ZnO) up to 18m^2/g (Pt/ZnO). Nevertheless, considering the experimental error of the technique and the low surface area of the catalysts, these differences could be negligible.

X-ray diffractogram of Pt/ZnO-175 (see supplementary information, Fig. S1A) showed a broad band at $2\theta = 46.7^\circ$ which can be ascribed to Pt^0 which, given the high platinum content (5% by weight), suggested a high dispersion of the metal. Subsequent reduction at 400 °C (Pt/ZnO-400) resulted in a shift of Pt^0 diffraction band to higher 2θ values, thus evidencing the formation of the Pt–Zn alloy as described by Ammari et al. [13].

TEM images of Pt/ZnO-175 and Pt/ZnO-400 solids (Fig. 1) confirmed the high dispersion of platinum, average particle diameter being 1.6 nm and 2.1 nm for Pt/ZnO-175 and Pt/ZnO-400, respectively.

Oxidation state of platinum (Pt^0, Pt^{2+} and Pt^{4+}) can be determined by XPS technique [20–22]. Therefore, metallic platinum exhibits binding energies of 70.7–70.9 and 74.0–74.2 eV for $4f_{7/2}$ and $4f_{5/2}$ electrons, respectively. In oxidized states, Pt^{2+} and Pt^{4+} exhibit much higher binding energies: 72.8–73.1 eV ($4f_{7/2}$) and 76.1–76.4 eV ($4f_{5/2}$) for Pt^{2+} and 74.0–74.9 eV ($4f_{7/2}$) and 77.3–78.2 eV ($4f_{5/2}$) for Pt^{4+}.

Pt (4f), Zn ($2p_{3/2}$) and Cl (2p) XPS profiles for as-synthesized system (Pt/ZnO-unred) as well as those of the solids reduced at 175 °C and 400 °C are shown in Fig. 2. Moreover, the most relevant features are summarized in Table 1. Unreduced solid exhibits two platinum species, with $Pt4f_{7/2}$ maxima at 72.7 and 74.7 eV. The former can be associated to Pt^{2+} whereas the latter can be ascribed to Pt^{4+}. In fact, its value is intermediate between that described for PtO_2 (74.0 eV) and $PtCl_4$ (75.1 eV) thus suggesting the presence of oxychlorinated Pt^{4+} species [23]. This is hardly surprising considering that H_2PtCl_6 was used as the platinum precursor. As regards Zn ($2p_{3/2}$) profiles, there are two Zn^{2+} peaks at 1021.6 eV and 1022.4 eV. The former is due to ZnO whereas the latter could be ascribed to oxychlorinated Zn^{2+} species [24]. Finally, in line with that described above, there are two Cl ($2p_{3/2}$) species at 198.2 eV and 199.7 eV [25,26] indicating the interaction with platinum and zinc, respectively.

Reduction at 175 °C (Pt/ZnO-175) results in the formation of Pt^0 (Pt ($4f_{7/2}$) peak at 70.9 eV) whereas some Pt^{2+} species remain (72.1 eV). More interestingly, there is an increase in the relative population of ZnOxCly species (see Table 1, relative intensities of Zn ($2p_{3/2}$) signal at 1022.4 eV and Cl ($2p_{3/2}$) at 199.7–199.9 eV) at

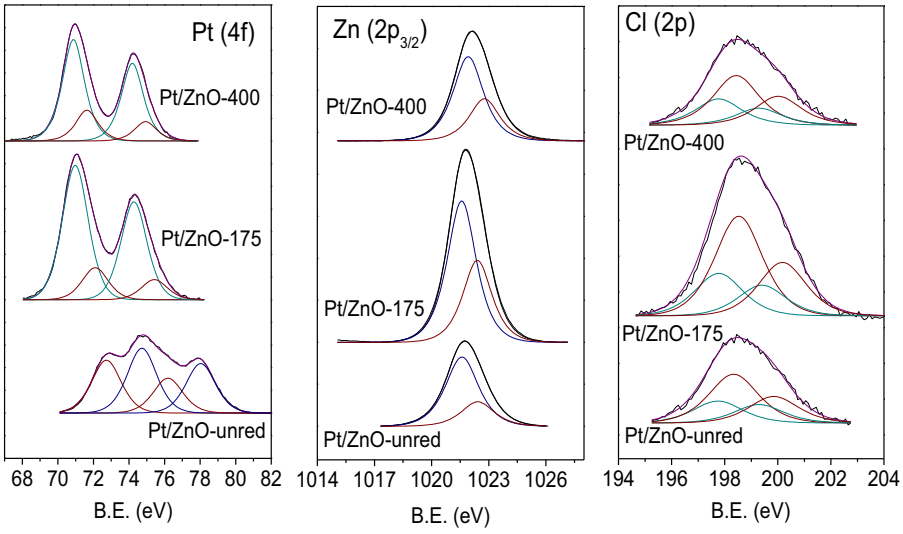

Fig. 2. XPS profiles in the Pt(4f), Zn(2p3/2) and Cl(2p) region of Pt/ZnO-unred, Pt/ZnO-175 and Pt/ZnO-400.

Table 1
Summary of XPS results.

Catalyst	Cl/Pt	Cl/Zn	Pt/Zn	BE Pt $4f_{7/2}$ (e.V.)	BE Zn $2p_{3/2}$ (e.V.)	BE Cl $2p_{3/2}$ (e.V.)
Pt/ZnO-unred	1.190	0.125	0.105	72.7 (44.8%), 74.7 (55.2%)	1021.6 (73.9%), ZnO 1022.4 (26.1%) ZnO_xCl_y	198.2 (31.0%), Pt–Cl 199.7 (69.0%) Zn–Cl
Pt/ZnO-175	1.924	0.133	0.069	70.9 (80.8%), 72.1 (19.2%)	1021.6 (63.3%), 1022.4 (36.7%)	198.2 (29.6%), 199.9 (70.4%)
Pt/ZnO-400	1.755	0.093	0.053	70.9 (77.3%), 71.7 (22.7%)	1021.6 (68.7%), 1022.4 (31.3%)	198.2 (35.0%), 199.7 (65.0%)

the expense of Pt–Cl species (decrease in the Cl ($2p_{3/2}$) signal at 198.2 eV). This seems to indicate that part of chlorine linked to Pt passed to the support.

When XPS results for Pt/ZnO-175 and Pt/ZnO-400 are compared, a decrease in total chlorine content on increasing reduction temperature from 175 to 400 °C is observed (drop in Cl/Zn ratio from 0.133 to 0.093). In fact, decomposition of $Pt(OH)_4(Cl)_2$ species with the release of HCl has been described in the literature [14] to proceed through the reaction:

$$[Pt(OH)_4(Cl)_2]^{2-} + 3H_2 \rightarrow Pt^0 + 4H_2O + 2HCl + 2e^-$$

Therefore, reduction of the catalyst results in a progressive loss of chlorine associated to platinum (coming from the precursor used, H_2PtCl_6) passing either to the support or being released as HCl. This is also accompanied by the progressive decoration of Pt particles by ZnO (see decrease in Pt/Zn ratio with reduction temperature at Table 1).

Catalytic performance of Pt/ZnO-unred, Pt/ZnO-175 and Pt/ZnO-400 for liquid-phase selective hydrogenation of crotonaldehyde to crotyl alcohol in water/dioxane (1:1 v/v) is summarized in Table 2. TOF values have been calculated considering particle sizes as determined by HAADF. As can be seen, reduction of Pt/ZnO at 175 °C resulted in a significant increase both in conversion and selectivity to unsaturated alcohol. Therefore, conversion values of 5.5% and 10.6% and selectivities of 54% and 95% were found for Pt/ZnO-unred and Pt/ZnO-175, respectively. Reduction at 400 °C led to a significant decrease in conversion (over 50%), whereas selectivity was hardly affected, TOF value decreasing from $2.0 \cdot 10^{-3}$ s^{-1} (Pt/ZnO-175) to $1.2 \cdot 10^{-3}$ s^{-1} (Pt/ZnO-400).

Increase in conversion and selectivity upon reduction at 175 °C could be ascribed both to the formation of Pt^0 (as evidenced by XRD and XPS) and the promotion of Pt–Zn interaction (SMSI, as evidenced by the decoration of Pt particles by ZnO). As for the reasons for the significant decrease in activity upon increasing reduction temperature from 175 °C up to 400 °C, there are three structural changes to be considered.

Firstly, as discussed above, reduction at 400 °C resulted in a slight increase in metal particle size from 1.6 to 2.1 nm. This change alone does not seem significant enough as to lead to such a change in conversion.

Secondly, reduction at 400 °C resulted in the formation of the Pt–Zn alloy, as evidenced by XRD and described by Ammari et al. [13]. The authors found that such an alloy is a key feature to obtain good selectivities to unsaturated alcohol. However, in our case selectivity values at 175 °C and 400 °C are quite similar (94–95%, Table 2) and X-ray diffractograms showed Pt–Zn alloy only for Pt/ZnO-400 system (accompanied by a narrowing of the Lorentzian half width of Pt ($4f_{7/2}$) line from 1.6 to 1.4 for Pt/ZnO-175 and Pt/ZnO-400, respectively) [15].

Table 2
Summary of catalytic performance of the different Pt/ZnO systems in liquid-phase selective hydrogenation of crotonaldehyde to crotyl alcohol (but-2-en-1-ol). Metal dispersion, platinum mean diameter and metal surface have also been included.

Catalyst	TOF ($10^{-3}s^{-1}$)	Conversion (%)	but-2-en-1-ol (%)	Dispersion (%)	dp (nm)	S_m (m^2/g)
Pt/ZnO-unred	–	5.5	54	–	–	–
Pt/ZnO-175	2.0	10.6	95	56	1.6	175
Pt/ZnO-400	1.2	4.7	94	43	2.1	133

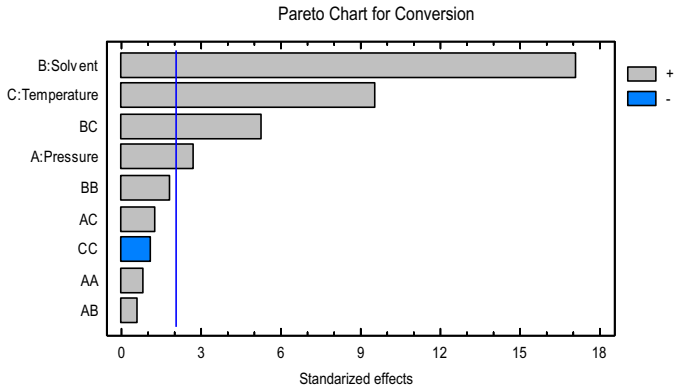

Fig. 3. Pareto chart for crotonaldehyde conversion.

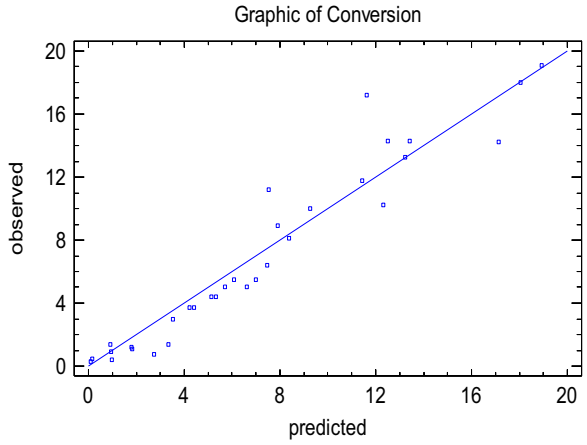

Fig. 5. Correlation between observed and predicted values for crotonaldehyde conversion.

Thirdly, as commented above, as Pt/ZnO is reduced, there is a progressive HCl release, thus leading to a decrease in total Cl species associated to both Pt and Zn. However, comparing relative populations of Cl ($2p_{3/2}$) at 198.2 eV and 199.7–199.9 eV (Pt–Cl and Zn–Cl interactions, respectively), upon reduction at 400 °C, decrease in

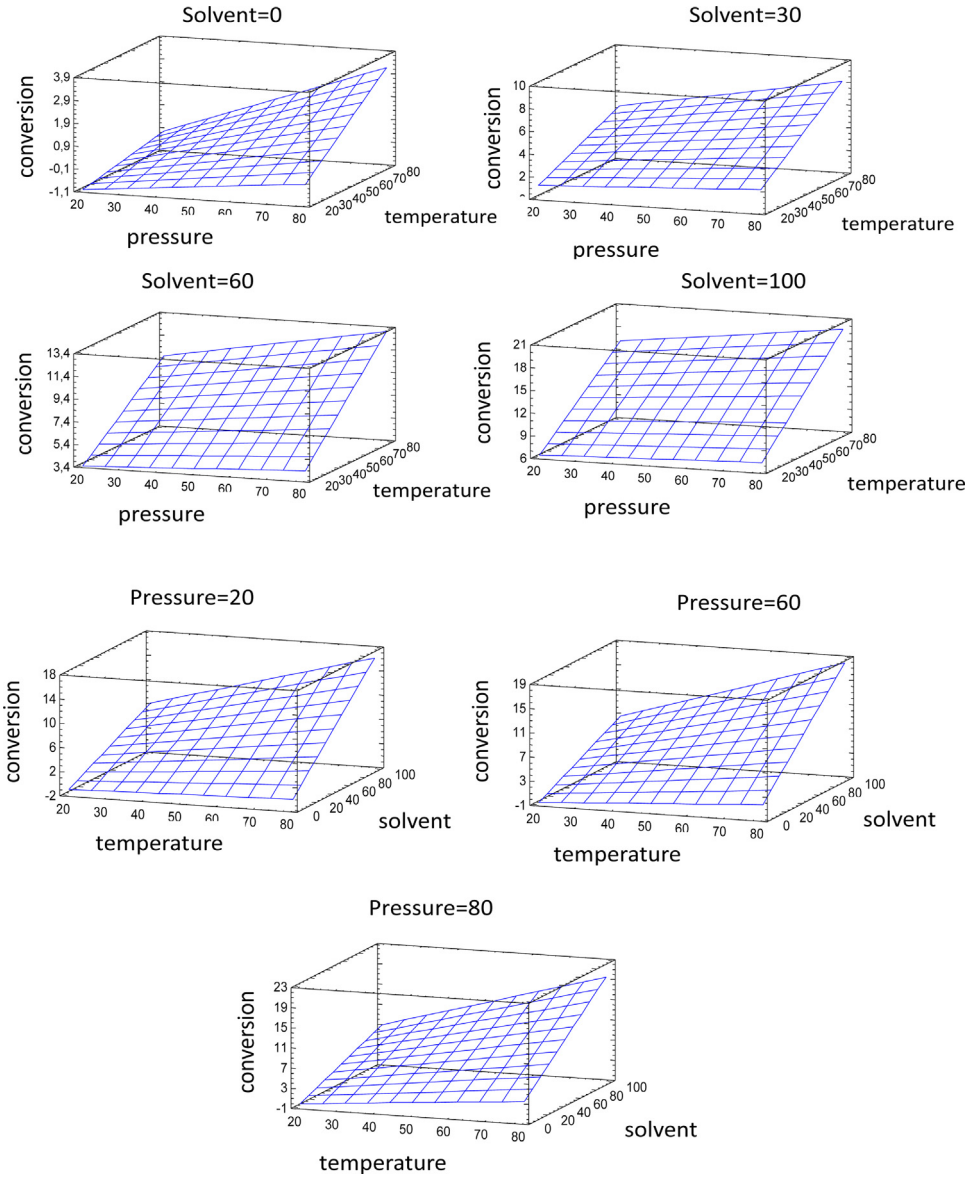

Fig. 4. Response surface plot for crotonaldehyde conversion.

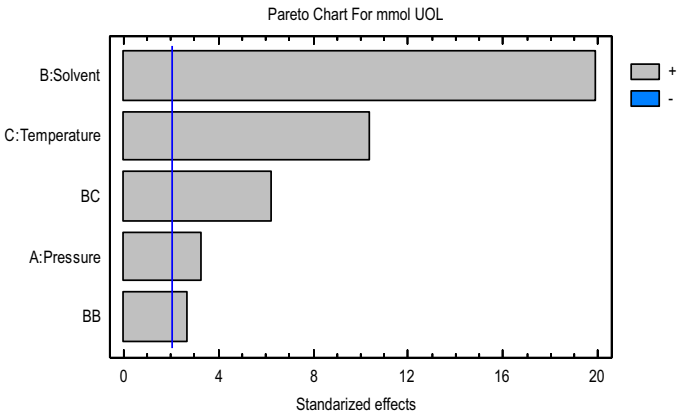

Fig. 6. Pareto chart for the yield of unsaturated alcohol (mmol of UOL, crotyl alcohol).

Cl linked to Zn is more important (Table 1). Therefore, observed decrease in activity could be explained as the result of the combined effect of the slight increase in particle size and higher decoration of Pt particles (thus leading to less surface Pt atoms) as well as the decrease in the number of ZnOxCly species in Pt vicinity which acts as Lewis acid sites for C=O adsorption. Again, it would be important to determine the extent of the importance of the evolution of ZnOxCly species on catalytic results. In this sense, subsequent studies on the reutilization of Pt/ZnO-175 catalyst under operation conditions optimized through factorial design, will cast further light on that.

3.2. Optimization of the process through factorial design

The most active solid (Pt/ZnO-175) was chosen for further optimization of operational parameters through factorial design in order to maximize both crotonaldehyde conversion and the amount of unsaturated alcohol produced (yield of but-2-en-1-ol). Obtained data were evaluated by ANOVA test at a significance level of 5%. Results are presented in Figs. 3–8 and Tables 3 and 4.

As regards crotonaldehyde conversion, solvent was found to be the most significant factor exhibiting a positive effect, followed by pressure-temperature and temperature-solvent interactions (Fig. 3). Equation found from the model was:

$$\text{Conv.}(\%) = -1.309 + 0.0440 * S + 0.000707 * P * T + 0.00151 * T * S$$

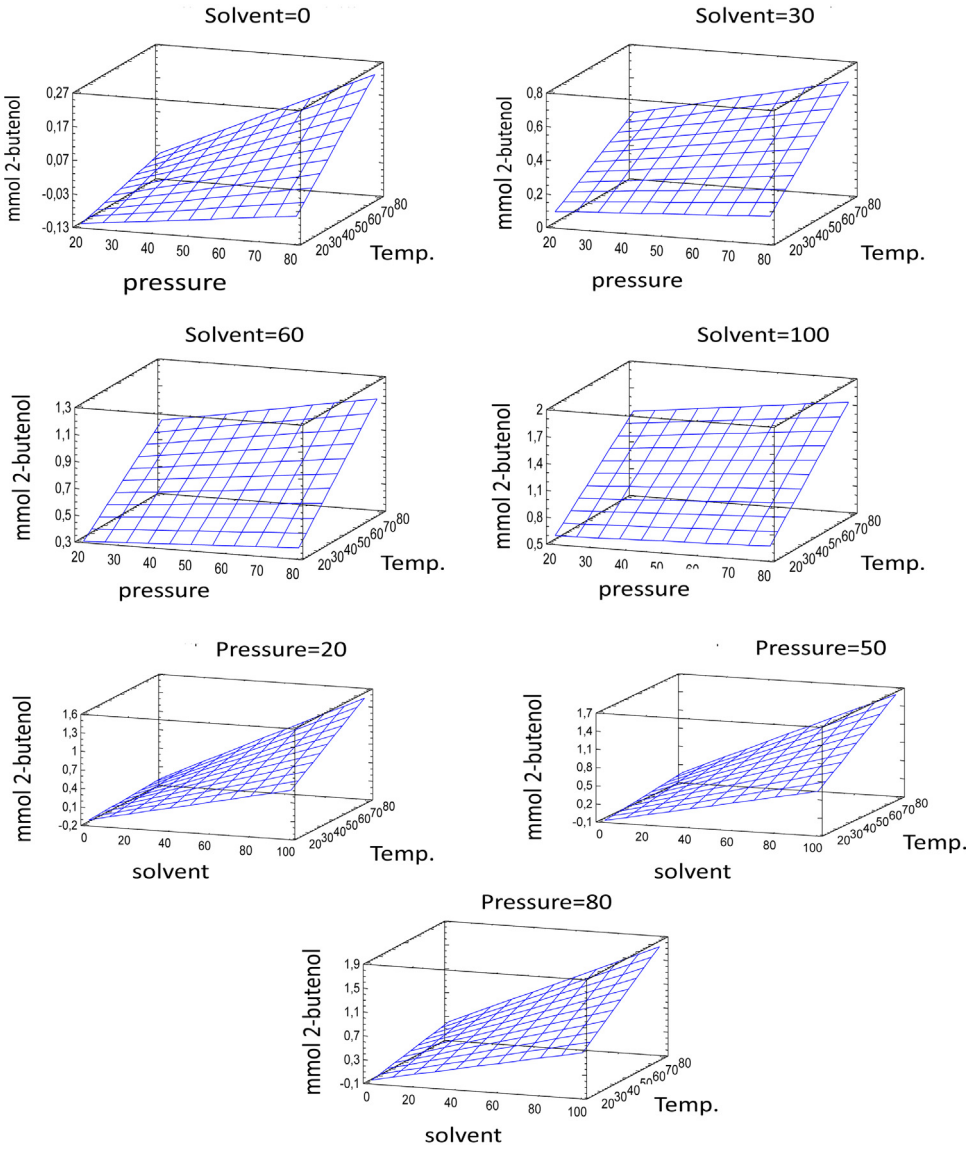

Fig. 7. Response surface plots for crotyl alcohol production (mmol of UOL).

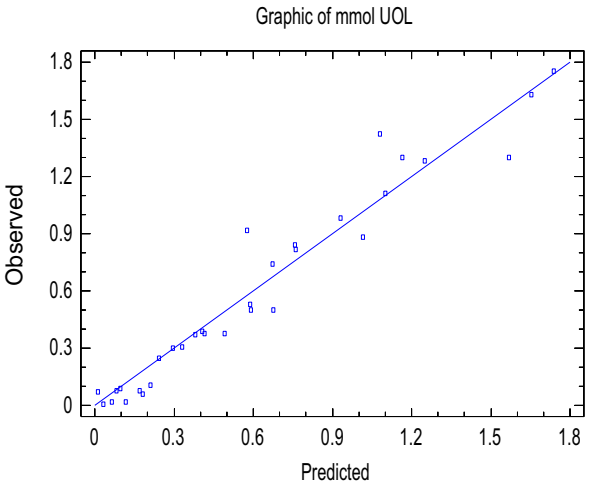

Fig. 8. Correlation between observed and predicted values for production of crotyl alcohol (mmol of UOL).

where solvent (S) is expressed in %water and pressure (P) and temperature (T) in psi and °C, respectively.

Influence of the different factors on conversion can be visualized in Fig. 4. As can be seen, as the water content increases and reaction conditions become more severe (higher temperature and pressures) conversion increases, the optimum value corresponding to 19.69% conversion for 100% water as the reaction medium, 80 psi initial pressure of hydrogen and 80 °C. Fig. 5 shows a good correlation between observed and predicted values ($r^2 = 0.95$) thus evidencing the validity of the model.

Similarly as for conversion, significant factors for but-2-en-1-ol production are solvent, pressure-temperature and solvent-temperature interactions (see Table 4 and Fig. 6). Equation for adjusted model is:

$$\text{But} - 2 - \text{en} - 1 - \text{ol(mmol)} = -0.144 + 0.00436 * \text{S} + 0.0000593 * \text{P} * \text{T} + 0.000134 * \text{S} * \text{T}$$

Again, response surfaces (Fig. 7) show that but-2-en-1-ol production increases with the water content and as temperature and hydrogen pressure rise, the effect of such variables decreasing in the order water content > temperature > > hydrogen pressure. A good correlation between experimental and predicted values ($r^2 = 0.94$) is obtained (Fig. 8) thus confirming again the validity of the model.

To sum up, optimization through factorial design has led to an improvement in but-2-enal conversion on Pt/ZnO-175 from 11% up to 19%, whereas selectivity to but-2-en-1-ol hardly changed, thus resulting in a 75% yield increase.

Table 3
Analysis of variance (ANOVA) for conversion.

Source	Sum of squares	df	Mean square	*F*-value	*P*-value
A: pressure	19.494	1	19.494	6.84	0.0136
B: solvent	772.359	1	772.359	271.13	0.0000
C: Temperature	241.174	1	241.174	84.66	0.0000
BC	73.7587	1	73.7587	25.89	0.0000
Total error	88.31	31	2.84871		
Total (corr.)	1195.1	35			

Table 4
Analysis of variance (ANOVA) for the yield of unsaturated alcohol (UOL, mmol).

Source	Sum of squares	df	Mean square	*F*-value	P-value
A: Pressure	0.175104	1	0.175104	10.78	0.0026
B: Solvent	6.42978	1	6.42978	395.95	0.0000
C: Temperature	1.755	1	1.755	108.07	0.0000
BB	0.117878	1	0.117878	7.26	0.0114
BC	0.638021	1	0.638021	39.29	0.0000
Total error	0.487169	30	0.016239		
Total (corr.)	9.60296	35			

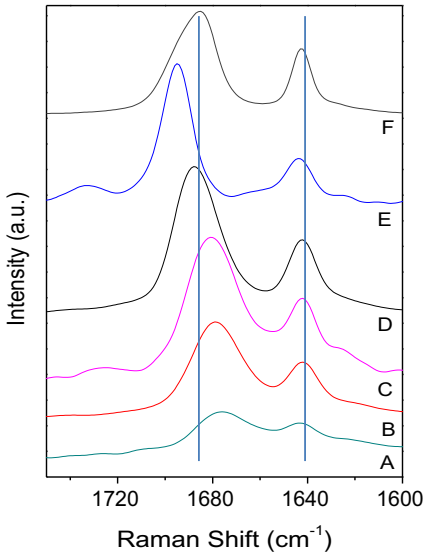

Fig. 9. FT-Raman of 0.5 M solutions of crotonaldehyde in different water/dioxane mixtures. Water content in the mixtures expressed as % (v/v) was 0% E, 30% (D), 50% (C), 70% (B) and 100%(A). F corresponds to the spectrum of pure crotonaldehyde.

3.3. Further studies on the solvent influence on catalytic results

All in all, solvent was found to be the most influential factor on both crotonaldehyde conversion and but-2-en-1-ol yield. In order to cast further light on the reason for that, solvent–substrate interaction was monitored through FT-Raman. Therefore, spectra of 0.5 M crotonaldehyde solutions in water, dioxane and water/dioxane mixtures (30%, 50% and 70% v/v) were registered.

Fig. 9 shows spectra in the 1600–1750 cm^{-1} region. The bands at 1640–1645 cm^{-1} are ascribed to C=C bond strectching [27]. As can be seen, the solvent has no influence on such a band, unless pure dioxane is used in which case a slight shift from 1642 to

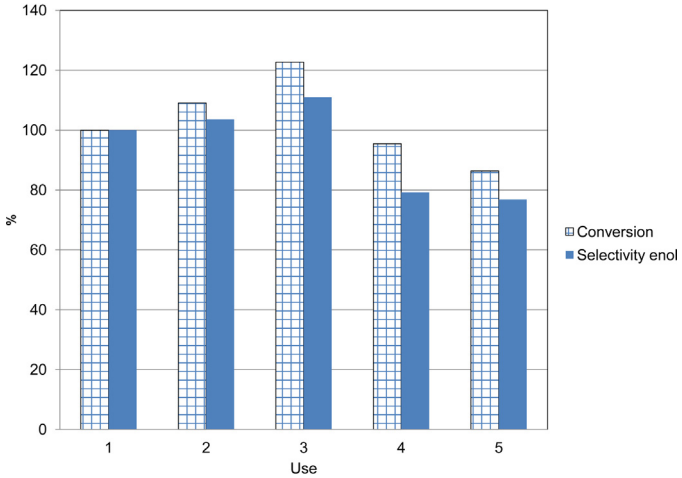

Fig. 10. Results obtained for reutilization experiments in liquid-phase selective hydrogenation of crotonaldehyde to but-2-en-1-ol on Pt/ZnO-175. Data corresponds to conversion and selectivity to but-2-en-1-ol as compared to the fresh catalyst (to which 100% conversion and selectivity had been assigned).

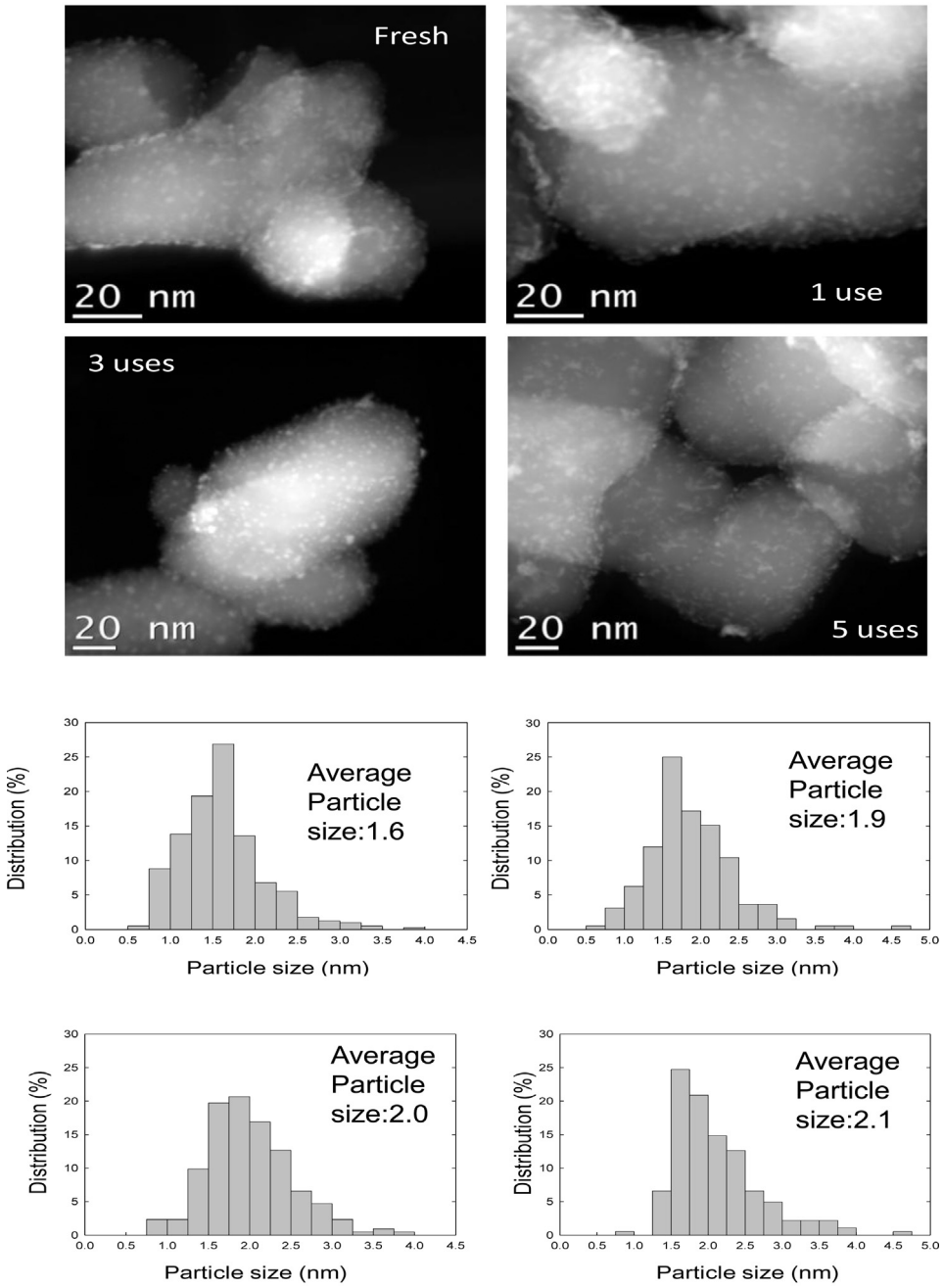

Fig. 11. HAADF images and Pt particle size distribution for Pt/ZnO-175 fresh and after 1, 3 and 5 uses.

1644 cm^{-1} is observed. On the contrary, the solvent has significant effects on the band at 1675–1695 cm^{-1}, which is associated to C=O bond stretching, appearing at wavenumbers below 1700 cm^{-1} as a result of conjugation [27,28]. Therefore, such a band appears at 1685 cm^{-1} for pure crotonaldehyde and shifts to higher frequencies (1695 cm^{-1}) for 0.5 M solutions of crotonaldehyde in pure dioxane, thus evidencing a shortening of carbonyl bond which thus becomes stronger. On the contrary, as water content increases, C=O band shifts to lower wavenumbers, thus evidencing a progressive weakening of C=O bond. Recently, a paper by Akpa et al. [29] on solvent effects in the hydrogenation of butan-2-one over a Ru/SiO_2 catalyst appeared. Using water/isopropyl alcohol mixtures as the solvent and combining DFT calculations and experimental data, the authors found that water could both lower activation energy and alter the hydrogenation mechanism, thus favoring the hydrogenation of C=O bond. These observations are consistent with our catalytic results: the higher the water content, the weaker the C=O bond thus favoring the selective reduction of this bond as compared to C=C and resulting in higher but-2-en-1-ol yields. However, high water contents complicate analyses since higher contents in reactant and products are found in the gas phase. In any case, results presented here consider the sum of both phases.

3.4. Studies on catalyst reutilization

Once reaction conditions had been optimized through factorial design (80 °C, 80 psi, pure water as the solvent), they were selected for experiments on reutilization of the catalyst. Catalyst regeneration consisted in washing with water first and then with dichloromethane. Finally, it was dried in a muffle furnace at 110 °C for 10 h before activation at 175 °C under hydrogen flow.

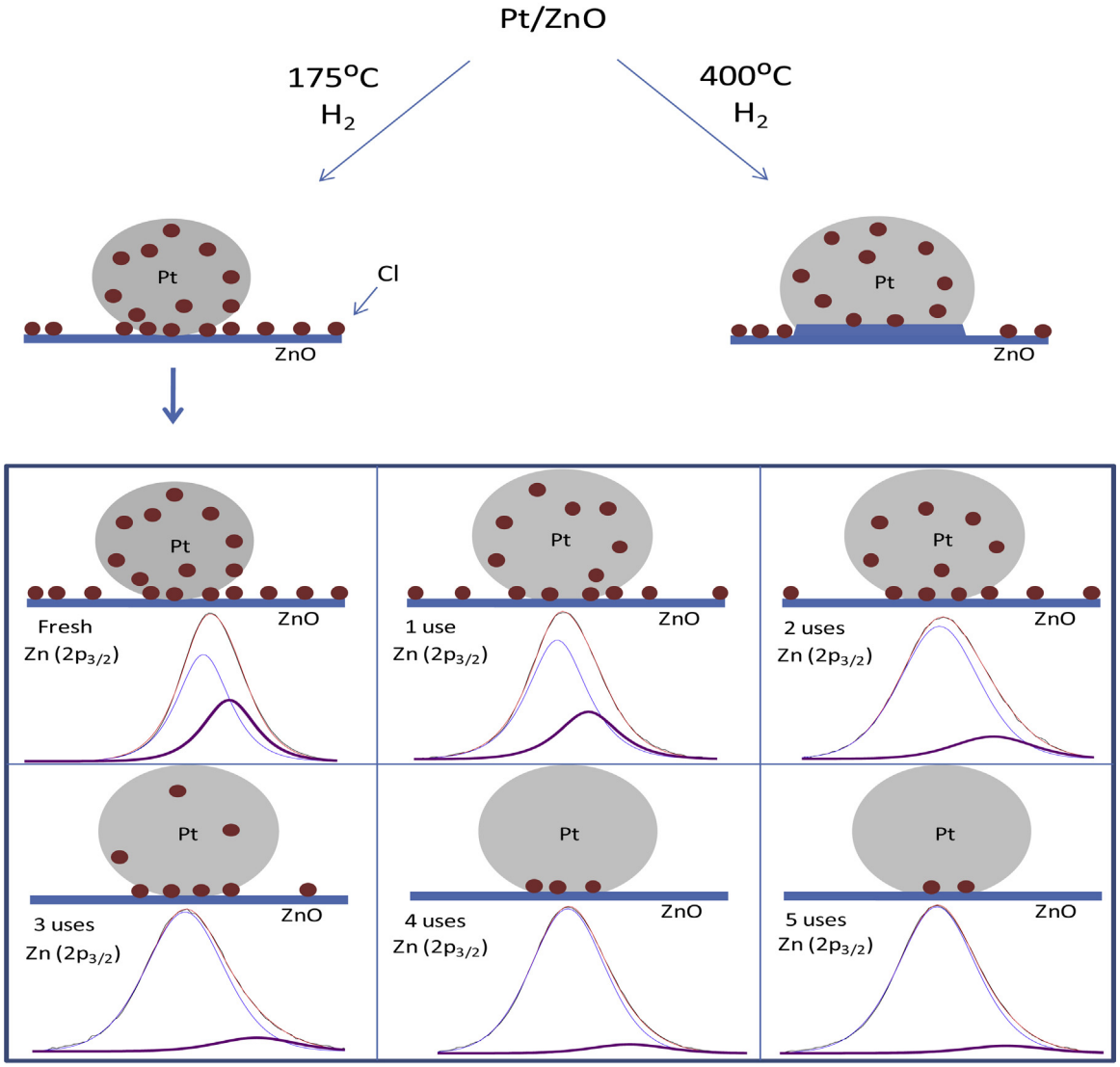

Fig. 12. Pictorial representation of structural changes in Pt/ZnO system reduction temperature and reuses of Pt/ZnO-175. Black balls represent Cl atoms.

Results found for reutilization essays are depicted in Fig. 10, using catalytic performance of fresh Pt/ZnO-175 as the reference (i.e. 100% conversion and 100% selectivity). As can be seen, there is a progressive increase in conversion and selectivity up to the third use whereas subsequent utilization results in a drop in both variables. In any case, conversion and selectivity values after five uses remain 86% and 76% its initial value, respectively.

In order to look for the reason for the observed catalytic behavior, reused systems were characterized by HAADF, XPS and XRD. HAADF (Fig. 11) shows an increase in platinum particle size after the first use whereas subsequent utilization leads to a reduction in the number of particles with particle sizes below 1.5 nm but average diameter remain ca. 2.0 nm. A narrowing of Pt^0 signal at ca. $2\theta = 46.7\square$ with the uses is observed in X-ray diffractograms (Fig. S2 in Supplementary Material) which, given the fact that mean particle size hardly changes, could be ascribed to an increase in crystallinity (probably as a result of progressive release of Cl associated to Pt).

Evolution of Zn ($2p_{3/2}$) and Pt (4f) signals with reutilization is depicted in Supplementary Figs. S3 and S4, respectively. Moreover, a pictorial representation of the structural changes in the catalyst inferred from XRD, HAADF and XPS evidences is given in Fig. 12.

Therefore, as regards Zn ($2p_{3/2}$) signal (Fig. 12 and Fig. S3 in Supplementary Material), reutilization results in a progressive decrease in the band associated to ZnOxCly species which is accompanied by a shift at higher binding energies. As the number of uses increases, there is a progressive loss of Cl content (either through leaching or release as HCl during catalyst activation). Pt acts as the chloride source and ZnOxCly species next to Pt are continuously regenerated, whereas regeneration of the further species is more difficult. Between the first and third use conversion and selectivity increases probably as a result of the progressive release of Cl linked to Pt atoms (in fact Cl is a well-known Pt-poison) [30,31] and the formation of ZnOxCly species next to the noble metal which acts as Lewis acids thus favoring C=O adsorption. However, at one point (third use) regeneration of ZnOxCly species is no longer possible as Cl on Pt atoms is scarce, thus leading to a progressive descend in ZnOxCly species and consequently resulting in the decrease in conversion and selectivity. One could think of the possibility of Pt leaching during reutilization essays. However, ICP-MS allowed us to rule out such possibility. In fact, the cumulative loss of platinum after five reuses is only 0.20% of the total platinum content.

4. Conclusions

Liquid-phase selective hydrogenation of crotonaldehyde to crotyl alcohol was studied on Pt/ZnO system. Factorial design of

experiments allowed us to evidence the significant effect of the water content on the solvent mixture on catalytic performance. Therefore, but-2-en-1-ol yield increases with the water content in water/dioxane mixtures. FT-Raman studies evidenced the weakening of C=O bond through hydrogen-bonding with water which favors its selective hydrogenation with respect to unaffected C=C bond in crotonaldehyde.

Reutilization studies confirmed the key role of ZnOxCly species close to Pt which acting as Lewis sites could favor anchoring of crotonaldehyde through C=O bond. As Pt/ZnO-175 is reused, there is a progressive loss of chlorine bonded to Pt (coming from the metal precursor, H_2PtCl_6) thus resulting in HCl release and generation of ZnOxCly species. Therefore, the latter species, responsible for the outstanding catalytic performance of Pt/ZnO-175, are regenerated and catalytic performance increases as Pt particles are less poisoned by Cl. However, at one point there is no enough Cl left as to pass from Pt particles to the support and compensate for the loss of ZnOxCly species, thus resulting in the loss of activity and selectivity.

Acknowledgments

The authors are thankful to Junta de Andalucia and FEDER funds (P08-FQM-3931 and P09-FQM-4781 projects).

Appendix A. Supplementary data

Supplementary material related to this article can be found, in the online version, at http://dx.doi.org/10.1016/j.apcatb.2014.02.023.

References

[1] P. Mäki-Arvela, J. Hájek, T. Salmi, D.Yu. Murzin, Appl. Catal. A 292 (2005) 1–49.
[2] U.K. Singh, M.A. Vannice, J. Catal. 199 (2001) 73–84.
[3] F. Ammari, C. Milone, R. Touroude, J. Catal. 235 (2005) 1–9.
[4] J. Kaspar, M. Graziani, G.P. Escobar, A. Trovarelli, J. Mol. Catal. 72 (1992) 243–251.
[5] R. Zheng, M.D. Porosoff, J.L. Weiner, S. Lu, Y. Zhu, J.G. Chen, Appl. Catal. A 419/420 (2012) 126–132.
[6] E.V. Ramos-Fernandez, A. Sepulveda-Escribano, F. Rodriguez-Reinoso, Catal. Commun. 9 (2008) 1243–1246.
[7] Z.G. Szabó, F. Solymosi in "Proceedings, 2nd International Congress on Catalysis", p. 1627, Technip, Paris, 1961.
[8] S.J. Tauster, S.C. Fung, R.L. Garten, J. Am. Chem. Soc. 100 (1978) 170–175.
[9] J. Hidalgo-Carrillo, M.A. Aramendia, A. Marinas, J.M. Marinas, F.J. Urbano, Appl. Catal. A 385 (2010) 190–200.
[10] J.C. Serrano-Ruiz, J. Luettich, A. Sepulveda-Escribano, F. Rodriguez-Reinoso, J. Catal. 241 (2006) 45–55.
[11] M. Abid, V. Paul-Boncour, R. Touroude, Appl. Catal. A 297 (2006) 48–59.
[12] A.M. Ruppert, T. Paryjczak, Appl. Catal. A 320 (2007) 80–90.
[13] F. Ammari, J. Lamotte, R. Touroude, J. Catal. 221 (2004) 32–42.
[14] M. Consonni, D. Jokic, D.Y. Murzin, R. Touroude, J. Catal. 188 (1999) 165–175.
[15] D. Wang, F. Ammari, R. Touroude, D.S. Su, R. Schloegl, Catal. Today 147 (2009) 224–230.
[16] A. Ruefer, W. Reschetilowski, Chem. Eng. Sci. 75 (2012) 364–375.
[17] C. Verdugo, D. Luna, A. Posadillo, E.D. Sancho, S. Rodriguez, F. Bautista, R. Luque, J.M. Marinas, A.A. Romero, Catal. Today 167 (2011) 107–112.
[18] M.M. Vdovenko, A.S. Demiyanova, T.A. Chemleva, I.Y. Sakharov, Talanta 94 (2012) 223–226.
[19] C. Fernandez, M.S. Larrechi, M.P. Callao, Talanta 79 (2009) 1292–1297.
[20] T. Teranishi, M. Hosoe, T. Tanaka, M. Miyake, J. Phys. Chem. B 103 (1999) 3818–3827.
[21] Y. Nagai, H. Shinjoh, K. Yokota, Appl. Catal. B 39 (2002) 149–155.
[22] V. Romanovskaya, M. Ivanovskaya, P. Bogdanov, Sens. Actuat. B 56 (1999) 31–36.
[23] C.D. Wagner, W.M. Riggs, L.E. Davis, J.F. Moulder, G.E. Muilenberg, Handbook of X-ray Photoelectron Spectroscopy, PerkinElmer Corporation (Physical Electronics), Minnesota, 1979.
[24] Y. Tanaka, H. Saito, Y. Tsutsumi, H. Doi, H. Imai, T. Hanawa, Mater. Trans. 49 (2008) 805–811.
[25] I. Fratoddi, E.S. Bronze-Uhle, A. Batagin-Neto, D.M. Fernandes, E. Bodo, C. Battocchio, I. Venditti, F. Decker, M.V. Russo, G. Polzonetti, C.F.O. Graeff, J. Phys. Chem. A 116 (2012) 8768–8774.
[26] E.L.D. Hebenstreit, W. Hebenstreit, H. Geisler, C.A. Ventrice Jr., D.A. Hite, P.T. Sprunger, U. Diebold, Surf. Sci. 505 (2002) 336–348.
[27] J. Michael Hollas, Modern spectroscopy, 4th Edition, John Wiley & Sons, Chichester, 2004, p. 161.
[28] D.W. Mayo, in: D.W. Mayo, F.A. Miller, R.W. Hannah (Eds.), Course notes on the interpretation of infrared and Raman spectra, John Wiley & Sons, New Jersey, 2003, p.18.
[29] B.S. Akpa, C. D'Agostino, L.F. Gladden, K. Hindle, H. Manyar, J. McGregor, R. Li, M. Neurock, N. Sinha, E.H. Stitt, D. Weber, J.A. Zeitler, D.W. Rooney, J. Catal. 289 (2012) 30–41.
[30] A. Wiersma, E. van de Sandt, M.A. den Hollander, H. van Bekkum, M. Makkee, J.A. Moulijn, J. Catal. 177 (1998) 29–39.
[31] Z.C. Zhang, B.C. Beard, Appl. Catal. A 174 (1998) 33–39.